DMD Fast Forward. Published on July 15, 2015 as DOI: 10.1124/dmd.115.065870
This article has not been copyedited and formatted. The final version may differ from this version.

DMD # 65870

The inhibition of human UDP-glucuronosyltransferase (UGT) enzymes by canagliflozin and dapagliflozin: Implications for drug-drug interactions

Attarat Pattanawongsa, Nuy Chau, Andrew Rowland and John O. Miners

Department of Clinical Pharmacology, Flinders University School of Medicine, Adelaide, Australia (AP, NC, AR, JOM)

Flinders Centre for Innovation in Cancer, Flinders University School of Medicine, Adelaide, Australia (AR, JOM)

Running title: UGT enzyme inhibition by canagliflozin and dapagliflozin

Address for correspondence:

Professor John O. Miners

Department of Clinical Pharmacology

Flinders University School of Medicine

Flinders Medical Centre

Bedford Park, SA 5042

Australia

Telephone: 61-8-82044131

Fax: 61-8-82045114

Email: john.miners@flinders.edu.au

Number of text pages (including table): 33

Number of figures: 4

Number of tables: 1

Number of references: 40

Number of supplemental tables: 6

Word counts:

Abstract, 249 words

Introduction, 747 words

Discussion, 1367 words

Abbreviations: BSA, bovine serum albumin (essentially fatty acid free); CNF, canagliflozin; DPF, dapagliflozin; DDI, drug-drug interaction; β-EST, β-estradiol; HLM, human liver microsomes; 4MU, 4-methylumbelliferone; PRO, propofol; SGLT2, sodium-glucose co-transporter 2; UGT, UDP-glucuronosyltransferase.

DMD Fast Forward. Published on July 15, 2015 as DOI: 10.1124/dmd.115.065870
This article has not been copyedited and formatted. The final version may differ from this version.

ABSTRACT

Canagliflozin (CNF) and dapaliflozin (DPF) are the first SGLT2 inhibitors to be approved for clinical use. Although available evidence excludes clinically significant inhibition of cytochromes P450, effects of CNF and DPF on human UDP-glucuronosyltransferase (UGT) enzymes are unknown. Here we report the inhibition of human recombinant UGTs by CNF and DPF, along with K_i values for selected recombinant and human liver microsomal UGTs. CNF inhibited all UGT1A subfamily enzymes, but greatest inhibition was observed with UGT 1A1, 1A9 and 1A10 (IC_{50} values ≤ 10 μM). DPF similarly inhibited UGT 1A1, 1A9 and 1A10, with IC_{50} values ranging from 39 – 66 μM. In subsequent kinetic studies, CNF inhibited recombinant and human liver microsomal UGT1A9; K_i values ranged from 1.4 - 3.0 μM, depending on the substrate (propofol/4-methylumbelliferone) - enzyme combination. K_i values for CNF inhibition of UGT1A1 were approximately 3-fold higher. Consistent with the activity screening data, DPF was a less potent inhibitor of UGT1A1 and UGT1A9. The K_i for DPF inhibition of UGT1A1 was 81 μM, while K_i values for inhibition of UGT1A9 ranged from 12 to 15 μM. Based on the in vitro K_i values and plasma concentrations reported in the literature, DPF may be excluded as a perpetrator of DDIs arising from inhibition of UGT enzymes but CNF inhibition of UGT1A1 and UGT1A9 in vivo cannot be discounted. Since the SGLT2 inhibitors share common structural features, notably a glycoside moiety, investigation of drugs in this class for effects on UGT to identify (or exclude) potential DDIs is warranted.

INTRODUCTION

Type 2 diabetes, which accounts for more than 90% of all cases of diabetes, is a chronic disease characterized by hyperglycaemia due to a progressive insulin secretory defect on the background of insulin resistance (American Diabetes Association, 2012). The microvascular changes that occur in patients with diabetes may cause retinopathy, neuropathy and chronic kidney disease. Further, type 2 diabetes associates with comorbidities such as hyperlipidaemia, hypertension and stroke. Consequently, type 2 diabetes results in significant morbidity and mortality, which in turn have important social and economic consequences. Indeed, it has been estimated that diabetes accounts for more than 10% of total worldwide healthcare costs for adults, and this is likely to increase into the future given the number of people with diabetes is increasing in all countries and has been projected to total almost 600 million by 2035 (International Diabetes Foundation, 2014).

Although metformin is the first-line drug for the treatment of type 2 diabetes, combination therapy with another agent is generally required to achieve and maintain recommended levels of glycaemic control (American Diabetes Association, 2012; Australian Medicines Handbook, 2014). While most antidiabetic drugs target insulin secretion or insulin action, modulation of glucose homeostasis provides an alternative approach to glycaemic control. The kidney plays a critical role in glucose homeostasis through the absorption of filtered glucose. Sodium-glucose co-transporters (SGLT) 1 and 2, located in the proximal convoluted tubule, are together responsible for almost all glucose reabsorption. Of these, the low-affinity high-capacity SGLT2 accounts for approximately 90% of glucose reabsorption under normal circumstances. Based on the early observation that phlorizin, a β-glucoside, inhibits SGLT 1 and 2 (Kinne and

Castaneda, 2011), a number of β-glycoside inhibitors that specifically inhibit SGLT2 and hence enhance urinary glucose excretion have been developed as antidiabetic agents.

Cangliflozin (CNF) and dapaliflozin (DPF) are the first SGLT2 inhibitors to be approved for clinical use. Both have been demonstrated to improve short-term outcomes in adults with type 2 diabetes (Plosker, 2012; Stenlof et al., 2013; Vasilakou et al., 2013). CNF and DPF are C-glucosides (Figure 1), and available evidence indicates that glucuronidation of the glucoside moiety is the major metabolic pathway of both compounds in humans. CNF is glucuronidated at the 2- and 3-hydroxyl groups of the glucoside rings; the respective glucuronides are referred to as M5 and M7 (Mamidi et al., 2014). The urinary excretion of M5 and M7 in patients with type 2 diabetes ranges from 7-10% and 21-32% of the administered dose, respectively (Devineni et al., 2013). It has been reported that CNF glucuronidation is catalyzed by UGT1A9 and UGT2B4 (Scheen, 2014), but actual data appear not to have been published.

Several glucuronides were observed following incubation of DPF with hepatocytes from various species (Obermeier et al., 2010). One of these, termed M15, was the major metabolite from human hepatocytes. Following administration of radiolabelled DNF to healthy volunteers, DNF plus M15 accounted for > 72% of total plasma radioactivity (Obermeier et al., 2010). A later report confirmed that M15, now identified as DPF 3-O-glucuronide, was formed by incubations of human liver, kidney and intestinal microsomes with UDP-glucuronic acid (UDPGA) (Kasichayanula et al., 2012). Rates of DPF 2-O-glucuronidation by human liver microsomes (HLM) and

kidney microsomes were < 5% those of DPF 3-O-glucuronide. Peak plasma concentrations of DPF 3-O-glucuronide measured following a single oral 50 mg dose of DPF ranged from approximately 1 µg/l in healthy subjects to 2 µg/l in type 2 diabetes patients with moderate to severe renal impairment (Kasichayanula et al., 2012). It has been reported that DPF 3-O-glucuronidation is catalyzed by UGT1A9 (Plosker, 2012; Kasichayanula et al., 2012 and 2014; Scheen, 2014). As with CNF, however, actual data relating to the involvement of UGT1A9 in DPF glucuronidation appear not to have been published.

IC_{50} values for DPF inhibition of the major drug metabolizing human liver microsomal cytochromes P450 exceed 45 µM (Obermeier et al., 2010), and CNF also appears not to inhibit P450 activities to a clinically significant extent (Ivokana, Product Information, 2013). However, no systematic investigations of the effects of CNF and DPF on human UDP-glucuronosyltransferase (UGT) enzymes have been reported. Thus, studies were undertaken here to characterize the inhibition of human recombinant UGTs and, based on the results of these screening studies, the inhibition kinetics of human liver microsomal UGT1A1 and UGT1A9. Whereas DPF was a 'modest' inhibitor of these enzymes, CNF was shown to be a potent inhibitor of UGT1A1 and UGT1A9 raising the possibility that this drug may potentially act as a perpetrator of metabolic inhibitory drug-drug interactions (DDIs).

MATERIALS AND METHODS

Materials

Alamethicin (from *Trichoderma viride*), bovine serum albumin (BSA; essentially fatty acid free), codeine, diclofenac, β-estradiol (β-EST), β-estradiol-3-β-D-glucuronide, hecogenin, 4-methylumbelliferone (4MU), 4-methylumbelliferone β-D-glucuronide, phenylbutazone, propofol (PRO), and UDP-glucuronic acid (sodium salt) were purchased from Sigma-Aldrich (Sydney, Australia); CNF and DPF from Selleck Chemicals (Houston, TX); and codeine 6-O-β-D-glucuronide from Toronto Research Chemicals (North York, ON, Canada). Fluconazole, lamotrigine and lamotrigine N2-β-D-glucuronide were a gifts from Pfizer Australia (Sydney, Australia) and the Wellcome Research Laboratories (Beckenham, UK), respectively. Supersomes expressing UGT2B4, UGT2B7, UGT2B15 and UGT2B17 and pooled HLM (150 donor pool; equal number of male and female donors) were purchased from Corning Gentest (Tewksbury, MA). Solvents and other reagents used were of analytical reagent grade.

Methods

HLM and recombinant human UGTs

Approval for the use of human liver tissue for in vitro drug metabolism studies was obtained from the Southern Adelaide Clinical Research Ethics Committee. HLM were activated by pre-incubation with the pore-forming agent alamethicin (50 µg/mg microsomal protein) prior to use in incubations, as described by Boase and Miners (2002).

DMD Fast Forward. Published on July 15, 2015 as DOI: 10.1124/dmd.115.065870
This article has not been copyedited and formatted. The final version may differ from this version.

Human UGT 1A1, 1A3, 1A4, 1A6, 1A7, 1A8, 1A9 and 1A10 cDNAs were stably expressed in a human embryonic kidney cell line (HEK293T) according to Uchaipichat et al. (2004). After growth to at least 80% confluence, cells were harvested and washed in phosphate-buffered saline. Cells were subsequently lysed by sonication using a Vibra Cell VCX 130 Ultrasonics Processor (Sonics and Materials, Newtown, CT, USA). Lysates were centrifuged at 12,000 g for 1 min at 4°C, and the supernatant fraction was separated and stored in phosphate buffer (0.1 M, pH 7.4) at -80°C until use. Given the lower expression of UGT 2B4, 2B7, 2B15 and 2B17 in HEK293 cells, Supersomes expressing these proteins were used for activity and inhibition studies.

CNF and DPF inhibition of recombinant UGT enzyme activities

Recombinant human UGT enzyme activities were determined in in the absence and presence of CNF or DPF (1, 10 and 100 μM). CNF and DPF stock solutions were prepared in DMSO such that the final concentration of solvent in incubations was 0.5% (v/v), which has a negligible or minor effect on most UGT activities (Uchaipichat et al., 2004). An equivalent volume of DMSO was included in control incubations. Effects of CNF and DPF on UGT 1A1, 1A3, 1A6, 1A7, 1A8, 1A9, 1A10, 2B7, 2B15 and 2B17 activities were measured using the non-selective UGT substrate 4MU as the probe. Incubations were performed at a 4MU concentration corresponding to the apparent K_m or S_{50} of each enzyme (Uchaipichat et al., 2004), according to the method described by Lewis et al. (2007). Protein concentrations and incubation time varied for each enzyme (Uchaipichat et al., 2004). Inhibition of UGT1A4 by CNF and DPF was assessed with lamotrigine as the probe substrate according to the method of Rowland et al. (2006), while effects on UGT2B4 activity

DMD Fast Forward. Published on July 15, 2015 as DOI: 10.1124/dmd.115.065870
This article has not been copyedited and formatted. The final version may differ from this version.

were determined with codeine as the substrate as described by Raungrut et al. (2010). Concentrations of lamotrigine and codeine used in the UGT1A4 and UGT2B4 inhibition screening studies corresponded to the respective K_m values for each substrate/pair; 1.5 mM for lamotrigine/UGT1A4 and 2.0 mM for codeine/UGT2B4. Positive control inhibitors were used in all inhibition screening experiments: hecogenin (UGT1A4 – 10 μM); niflumic acid (UGT1A9 – 2.5 μM, UGT1A1 – 100 μM); phenylbutazone (UGT 1A3, 1A6, 1A7, 1A8, 1A10 – 500 μM); fluconazole (UGT 2B4 and 2B7 – 2.5 mM); and diclofenac (UGT 2B15 and 2B17 – 500 μM). The magnitude of inhibition of each positive control inhibitor (data not shown) was as expected from previous studies in this laboratory (Uchaipichat et al., 2004, 2006a and b; Raungrut et al., 2010; Miners et al., 2011). Within- and between-day coefficients for all activity assays, including with HLM as the enzyme source (see below), were < 5% and 10%, respectively.

Kinetic characterization of CNF and DPF inhibition of recombinant and human liver microsomal UGT 1A1 and 1A9 activities.

The kinetics and mechanisms of CNF and DPF inhibition of recombinant and human liver microsomal UGT1A1 and UGT1A9 were determined using β-EST and PRO/4MU as the respective probe substrates (Uchaipichat et al., 2004; Miners et al., 2010a). Incubation conditions and analytical procedures used to quantify β-EST, 4MU and PRO glucuronidation were as described in Miners et al. (2011). As with the inhibition screening studies, CNF and DPF were added to incubations in DMSO such that the final concentration was 0.5% v/v.

UGT1A1. Experiments to determine the inhibitor constants with UGT1A1 (0.25 mg/ml HEK293 cell lysate) as the enzyme source included four added CNF (3, 6, 9 and 12 μM) or DPF (30, 60, 90 and 120 μM) concentrations at each of three added β-EST (3, 6, and 15 μM) concentrations. Similarly, studies with pooled HLM (0.25 mg/ml) employed four added concentrations of CNF (15, 30, 45 and 90 μM) or DPF (30, 60, 90 and 120 μM) at each of the three added β-EST concentrations specified above.

UGT1A9. Experiments to characterize CNF and DPF inhibition of recombinant UGT1A9 followed the approach described for UGT1A1, except that 4MU and PRO were used as the substrates. The HEK293 cell lysate content of incubations were 0.025 mg/ml (4MU as substrate) or 0.25 mg/ml (PRO as substrate). The effects of four added CNF (30, 60, 90 and 120 μM) or DPF (45, 90, 135 and 180 μM) concentrations were investigated at each of three 4MU concentrations (8, 16 and 32 μM). Similarly, the effects of four added CNF (15, 30, 45 and 60 μM) or DPF (45, 90, 135 and 180 μM) concentrations were investigated at each of three PRO concentrations; 2, 4 and 8 μM with CNF as inhibitor, and 10, 15 and 20 μM with DPF as the inhibitor. Inhibition experiments with HLM (0.5 mg/ml) employed only PRO as the probe substrate, since 4MU is glucuronidated by multiple UGT enzymes. Experiments employed four added CNF (30, 60, 90 and 120 μM) or DPF concentrations (80, 150, 220 and 300 μM) at each of three added PRO concentrations (10, 25 and 50 μM). In addition, incubations contained BSA, either 0.5% (CNF) or 1% (DPF) w/v, since measurement of optimal UGT1A9 activity (recombinant and human liver microsomal) requires the presence of BSA to sequester inhibitory long-chain unsaturated fatty acids (see Results and Discussion sections). Binding of CNF,

DPF, β-EST, 4MU and PRO to enzyme sources and, where relevant, to BSA was corrected for in the calculation of inhibitor constants (i.e. expressed as $K_{i,u}$) for inhibition of UGT1A1 and UGT1A9 (see Results).

Measurement of the binding of CNF, DPF, β-EST, 4MU and PRO to HEK293 cell lysate, HLM and BSA

The binding of DPF to HEK293 cell lysate (0.025 and 0.25 mg/ml) and HLM (0.25 and 0.5 mg/ml), in the absence and presence of BSA where indicated, was performed over the concentration range shown in Supplemental Table 1 using a commercial rapid equilibrium dialysis (RED) device (Thermo Scientific, Rockford, IL). The sample chamber contained the enzyme source (± BSA, 0.5 or 1% w/v) and DPF (in DMSO, final concentration 0.5% v/v) in phosphate buffer (0.1 M, pH 7.4) while the buffer chamber side contained only phosphate buffer. Respective volumes of the sample and buffer chambers were 400 and 600 µl. Dialysis experiments were performed for 8 hr. Attainment of equilibrium was demonstrated using enzyme – enzyme (HLM or HEK293 cell lysate) and buffer – buffer controls at the lowest and highest DPF concentrations investigated in each experiment.

In contrast to DPF, dialysis was not achieved with CNF in enzyme – enzyme and buffer – buffer controls over 8 hr using the commercial RED device. However, equilibrium was achieved over this time using conventional equilibrium dialysis (employing dialysis cells). Thus, the binding of CNF to HEK293 cell lysate (0.025 and 0.25 mg/ml) and HLM (0.25 and 0.5 mg/ml), in the absence and presence of BSA where indicated, was performed over the concentration range shown in Supplemental Table 2 according to the procedure of McLure et al. (2000) using Dianorm

DMD Fast Forward. Published on July 15, 2015 as DOI: 10.1124/dmd.115.065870
This article has not been copyedited and formatted. The final version may differ from this version.

equilibrium dialysis cells (Dianorm, Munich, Germany) of 1.2 ml capacity per side, separated by Spectrapor number 4 dialysis membrane (molecular mass cut-off 12 – 14 kD; Spectrum Medical Industries Inc, Los Angeles, CA). One cell contained the enzyme source (± BSA, 0.5 or 1% w/v) and CNF (in DMSO, final concentration 0.5% v/v) in phosphate buffer (0.1 M, pH 7.4), and the other phosphate buffer alone. The dialysis cell assembly was immersed in a water bath at 37º C and rotated at 12 rpm for 8 hr.

The potential effects of CNF and DPF on the binding of β-EST, 4MU and PRO to enzyme sources (HEK293 cell lysate and HLM), in the absence and presence of BSA as appropriate, was assessed over the concentration ranges shown in Supplemental Tables 3 – 5. β-EST and 4MU binding was measured using the commercial RED device and conditions described for DPF (above). Like CNF, equilibrium was not established in enzyme – enzyme and buffer – buffer controls over 8 hr for PRO using the RED device. However, equilibrium was attained within 8 hr using conventional equilibrium dialysis. Thus, the binding of PRO to incubation constituents was determined as described for CNF.

Following dialysis, an aliquot from each chamber of the RED device or Dianorm equilibrium dialysis cell was treated with 4 volumes of ice-cold methanol containing 4% glacial acetic acid and centrifuged (5,000 *g* for 10 min). Concentrations of CNF, DPF, β-EST, 4MU and PRO were measured by HPLC using the chromatography conditions given in Supplemental Table 6. The fraction unbound of each compound to incubation constituents (HEK293 cell lysate, HLM and BSA), fu_{inc}, was calculated as

DMD Fast Forward. Published on July 15, 2015 as DOI: 10.1124/dmd.115.065870
This article has not been copyedited and formatted. The final version may differ from this version.

the concentration of the compound in the buffer cell divided by the concentration in the sample cell.

Data Analysis

All kinetic and inhibition experiments were performed in duplicate and data points represent the mean of duplicate estimates (<10% variance). $K_{i,u}$ values for CNF and DPF inhibition of recombinant and human liver microsomal UGT1A9 activities were determined by fitting the expressions given in equations 1 to 3 to experimental data using Enzfitter (version 2.0, Biosoft, Cambridge, UK), while $K_{i,u}$ values for CNF and DPF inhibition of recombinant and human liver microsomal UGT1A1 activities were determined by fitting the expressions given in equations 4 and 5 to experimental data. Goodness of fit of all expressions was assessed from comparison of the parameter SE of fit, coefficient of determination (r^2), 95% confidence intervals, and F-statistic.

Equation 1, competitive inhibition:

$$v = \frac{V_{max} \times [S]}{K_m(1+[I]/K_i)+[S]}$$

where V_{max} is maximal velocity, [S] is substrate concentration, K_m is the Michaelis constant, [I] is the inhibitor concentration, and K_i is the inhibitor constant (for the EI complex).

Equation 2, non-competitive inhibition:

$$v = \frac{V_{max} \times [S]}{(1+[I]/K_i)(K_m+[S])}$$

where K_i is the inhibitor constant for the EI and ESI complexes.

Equation 3, mixed (competitive – non-competitive) inhibition:

$$v = \frac{V_{max} \times [S]}{K_m(1+[I]/K_i)+[S](1+[I]/K_i')}$$

DMD Fast Forward. Published on July 15, 2015 as DOI: 10.1124/dmd.115.065870
This article has not been copyedited and formatted. The final version may differ from this version.

where K_i and K_i' are the inhibitor constants for the EI and ESI complexes, respectively.

Equation 4, competitive inhibition of an enzyme exhibiting sigmoidal kinetics (homotropic positive cooperativity), version 1:

$$v = \frac{V_{max} \times {S_{50}}^n}{{S_{50}}^n \left(1 + \frac{[I]}{K_i}\right) + S^n}$$

where S_{50} is the concentration at half V_{max} and n is the Hill coefficient.

Equation 5, competitive inhibition of an enzyme exhibiting sigmoidal kinetics (homotropic positive cooperativity), version 2:

$$v = \frac{V_{max} \times {S_{50}}^n}{{S_{50}}^n \left(1 + \frac{[I]}{K_i}\right)^n + S^n}$$

Equation 6, ratio of the areas under the plasma concentration – time curve (AUC) of the victim drug in the absence and presence of the inhibitor:

$$\frac{AUC_i}{AUC} = \frac{1}{\frac{f_m}{1+[I]/K_i} + (1 - f_m)}$$

where f_m is the fraction of the dose metabolized by the enzyme and pathway of interest.

Equation 7, hepatic inlet concentration of inhibitor:

$$[I_{inlet}] = [I_{max}] + \frac{k_a \times F_a \times Dose}{Q_H}$$

where $[I_{max}]$, k_a, F_a, and Q_H are the maximum drug concentration in the systemic circulation associated with a given dose, absorption rate constant, fraction absorbed from the gastrointestinal tract and liver blood flow, respectively.

DMD Fast Forward. Published on July 15, 2015 as DOI: 10.1124/dmd.115.065870
This article has not been copyedited and formatted. The final version may differ from this version.

RESULTS

CNF and DPF inhibition of recombinant human UGT enzymes

CNF inhibited all UGT1A subfamily enzymes with IC_{50} values < 50 µM (Figure 2). Greatest inhibition was observed with UGT 1A1, 1A9 and 1A10, with respective IC_{50} values of 10, 6 and 7 µM. Inhibition of UGT 2B7 and 2B15 was 'moderate' (IC_{50} values approximately 50 µM), whereas CNF had a negligible effect on UGT 2B4 and 2B17 activities. Like CNF, DPF most potently inhibited UGT 1A1, 1A9 and 1A10. However, IC_{50} values (39 – 66 µM) were approximately 6-fold higher than those for CNF inhibition of these enzymes. Estimated IC_{50} values for DPF inhibition of all other UGT enzymes ranged from 75 – 3,500 µM.

It is known that recombinant and human liver microsomal UGT1A9, but not UGT1A1, activities are under-estimated in the absence of BSA due (see Discusson). Thus, experiments undertaken to characterize the inhibition kinetics of recombinant and human liver microsomal UGT1A9 included BSA in the incubation medium. The binding of CNF to albumin is extensive and, due to limitations of assay sensitivity, the concentration of BSA added to incubations containing CNF was 0.5% w/v. The somewhat less extensive binding of DPF to albumin permitted kinetic experiments to be performed in the presence of 1% w/v BSA. Experience in this laboratory indicates that the optimal effect of BSA on UGT activities occurs for concentrations in the range 0.5 to 2% w/v (for example Rowland et al., 2007 and 2008).

Binding of CNF and DPF to HEK293 cell lysate and HLM, with and without BSA

The binding of CNF and DPF to HEK293 cell lysate and to HLM was determined in the absence and presence of BSA. Data are shown in Supplemental Tables 1 and 2.

DMD Fast Forward. Published on July 15, 2015 as DOI: 10.1124/dmd.115.065870
This article has not been copyedited and formatted. The final version may differ from this version.

The non-specific binding of CNF and DPF to each enzyme source (± BSA) was concentration independent over the ranges studies. The mean fu_{inc} values for DPF binding to HLM and HEK293 cell lysate (both 0.25 mg/ml) in the absence of BSA (UGT1A1 inhibition studies) were 0.86 and 0.94, respectively (Supplemental Table 1). Mean fu_{inc} values for DPF binding to HEK293 cell lysate and HLM in the presence of BSA (1% w/v) ranged from 0.27 to 0.30. Addition of concentrations of β-EST, 4MU and PRO at the upper end of the ranges used in inhibition experiments did not affect DPF binding.

Similar trends were observed with CNF binding, although binding of CNF to enzyme sources and BSA (0.5% w/v) was higher than for DPF (Supplemental Table 2). The mean fu_{inc} values for CNF binding to HLM and HEK293 cell lysate (both 0.25 mg/ml) in the absence of BSA (UGT1A1 inhibition studies) were 0.38 and 0.96, respectively (Supplemental Table 2). When BSA (0.5% w/v) was added to suspensions of HEK293 cell lysate (0.025 and 0.25 mg/ml) and HLM (0.5 mg/ml) (UGT1A9 inhibition studies), CNF binding increased substantially; mean fu_{inc} values were 0.08 to 0.12. As with DPF, addition of concentrations of β-EST, 4MU and PRO at the upper end of the ranges used in inhibition experiments did not affect CNF binding.

It was further demonstrated that concentrations of CNF and DPF at the upper end of the ranges used in inhibition experiments did not affect 4MU binding to HEK293 cell lysate plus BSA, and PRO binding to HEK293 cell lysate and HLM plus BSA (UGT1A9 inhibition experiments) (Supplemental Tables 3 and 4). Similarly, concentrations of CNF and DPF at the upper end of the ranges used in inhibition

DMD Fast Forward. Published on July 15, 2015 as DOI: 10.1124/dmd.115.065870
This article has not been copyedited and formatted. The final version may differ from this version.

experiments did not affect the binding of β-EST binding to HEK293 cell lysate and HLM (UGT1A1 inhibition experiments) (Supplemental Table 5).

Binding of CNF, DPF, β-EST, 4MU and PRO to enzyme sources and, where relevant, to BSA was corrected for in the calculation of $K_{i,u}$ values for inhibition of UGT1A1 and UGT1A9 (below).

Kinetics of CNF and DPF inhibition of recombinant and human liver microsomal UGT1A1 and UGT1A9

β-EST was used as the UGT1A1 probe substrate, both for the recombinant and human liver microsomal enzymes. β-EST 3-glucuronidation by recombinant UGT1A1 exhibits sigmoidal kinetics, with an S_{50} of 10 μM (Udomuksorn et al., 2007). It was confirmed here that β-EST 3-glucuronidation by HLM also exhibits sigmoidal kinetics, with an S_{50} of 14 μM (data not shown). Experimental data for inhibition of β-EST 3-glucuronidation by CNF and DPF were poorly fit by the expressions for competitive, non-competitive and mixed inhibition (equations 1 – 3, Data Analysis), presumably because the concentrations of β-EST employed in the inhibition experiments (3, 6 and 15 μM) spanned the S_{50} and therefore included the early curved and pseudo-linear sections of the sigmoidal substrate concentration versus velocity plots. Thus, we modified the Hill equation, which describes sigmoidicity, to include an inhibition term analogous to the equation for competitive inhibition of an enzyme exhibiting Michaelis-Menten kinetics (equation 1, Data Analysis). Both derived equations (equations 4 and 5, Data Analysis) described CNF and DPF inhibition of UGT1A1 well, both visually and statistically. However, equation 5 gave marginally improved fits statistically (Figures 3 and 4); F-statistic > 4,980, $r^2 = 0.999$, and

standard error of parameter fits < 5%. By contrast, experimental data for CNF and DPF inhibition of recombinant UGT1A9 (4MU and PRO as substrates) and human liver microsomal UGT1A9 (PRO as substrate) were well described by the equation for competitive inhibition of an enzyme exhibiting Michaelis-Menten kinetics (equation 1).

Kinetic plots for CNF and DPF inhibition are shown in Figures 3 and 4, respectively, and derived $K_{i,u}$ values are given in Table 1. CNF was a potent inhibitor of recombinant and human liver microsomal UGT1A9, with $K_{i,u}$ values in the range 1.4 to 3.0 µM, depending on the substrate/enzyme combination. $K_{i,u}$ values for CNF inhibition of UGT1A1 were approximately 3-fold higher. Consistent with the activity screening data, DPF was a less potent inhibitor of UGT1A1 and UGT1A9. The $K_{i,u}$ for inhibition of UGT1A1 by both compounds was 81 µM, while $K_{i,u}$ values for inhibition of UGT1A9 ranged from 12 to 15 µM.

DMD Fast Forward. Published on July 15, 2015 as DOI: 10.1124/dmd.115.065870
This article has not been copyedited and formatted. The final version may differ from this version.

DISCUSSION

CNF and DPF are the first SGLT2 inhibitors to be approved for clinical use. Since many patients with type 2 diabetes present with multiple co-morbidities, polypharmacy is common highlighting the need to carefully evaluate potential DDIs. FDA guidelines now recommend that new drugs are evaluated for their potential to inhibit the major human drug metabolizing cytochrome P450 and UGT enzymes in vitro in order to assess their potential role as perpetrators of inhibitory DDIs (www.fda.gov/downloads/drugs/guidancecomplianceregulatory information/guidances/ucm292362.pdf). As noted in the Introduction, it has been reported that IC_{50} values for DPF inhibition of the major drug metabolizing human liver microsomal P450 enzymes exceed 45 µM (Obermeier et al., 2010), and the Product Information for CNF indicates a low propensity for inhibition of P450 enzyme activities (Ivokana, Product Information, 2013). However, no systematic investigations of the effects of CNF and DPF on human UGT enzymes have been reported. Here we demonstrate that CNF is a potent inhibitor of UGT1A1 and UGT1A9 in vitro, whereas DPF inhibition of these enzymes is 'moderate'. UGT 1A1 and 1A9 are both expressed in liver, while UGT1A9 is additionally expressed in kidney. Hence, inhibition of UGT 1A1 and 1A9 may potentially result in the reduced clearance of drugs, non-drug xenobiotics, and endogenous compounds that are eliminated by these enzymes.

Long-chain unsaturated fatty acids released from the microsomal membrane during the course of an incubation are known to inhibit UGT1A9, but not UGT1A1, activity resulting in over-estimation of the K_m and K_i values of substrates and inhibitors of this enzyme, respectively (Rowland et al., 2008; Gill et al., 2012; Manevski et al, 2011;

DMD Fast Forward. Published on July 15, 2015 as DOI: 10.1124/dmd.115.065870
This article has not been copyedited and formatted. The final version may differ from this version.

Walsky et al., 2012). Thus, experiments to determine $K_{i,u}$ values for CNF and DPF glucuronidation of recombinant and human liver microsomal UGT1A9 were undertaken in the presence of BSA, which sequesters the inhibitory fatty acids thereby providing a more accurate value of the inhibitor constant. $K_{i,u}$ values for CNF and DPF inhibition of human liver microsomal and recombinant UGT1A9 were determined with PRO, which is a selective substrate for this enzyme (Miners et al., 2010a). Inhibition of recombinant UGT1A9 was also investigated with 4MU as the probe substrate. Although 4MU is a non-selective UGT substrate, the intrinsic clearance for 4MU glucuronidation by UGT1A9 is very high (Uchaipichat et al., 2004), and it is therefore a valuable substrate for measuring the activity of the recombinant enzyme. $K_{i,u}$ values for CNF inhibition of recombinant and human liver microsomal UGT1A9 with the three enzyme/substrate combinations were close in value (1.4 - 3.0 μM), as were $K_{i,u}$ values for DPF inhibition of each of the enzyme/substrate combinations (12 - 15 μM) (Table 1). There was also close agreement in the $K_{i,u}$ values for CNF (7.2 – 9.1 μM) and DPF (81 μM) inhibition of recombinant and human liver microsomal UGT1A1, which were determined using the selective substrate β-EST (Miners et al., 2010a).

The propensity of a compound to act as a perpetrator of inhibitory DDIs may be assessed using equation 6 (Data analysis) (Ito et al., 1998; Miners et al., 2010b), where the key term is the $[I]/K_i$ ratio. For a victim drug completely metabolized along a single metabolic pathway by a single enzyme, $f_m = 1$ and equation 6 simplifies to the expression AUC-ratio = $(1 + [I]/K_i)$. In the absence of data which allows calculation of the hepatic input concentration (i.e. k_a and/or F_a), the inhibitor concentration is

generally taken as the maximum plasma unbound concentration of the putative perpetrator (for example, Raungrut et al., 2010).

The reported mean maximum plasma concentrations of CNF at steady-state for doses of 100 mg/day and 300 mg/day (the highest recommended dose) are 1,227 µg/L (2.8 µM) and 4,678 µg/l (10.7 µM), respectively (Devineni et al., 2013). These concentrations are similar to or exceed the $K_{i,u}$ values observed for CNF inhibition of UGT1A9 (1.4 – 3.0 µM) and UGT1A1 (7.2 – 9.1 µM). Based on these CNF plasma concentrations and $K_{i,u}$ values, approximate 30 – 40% and 215 – 245% increases in the AUC-ratio for exclusive UGT1A1 substrates are predicted for the 100 and 300 mg/day doses, respectively, using the simplified equation given above. For exclusive UGT1A9 substrates, predicted AUC-ratio increases range from 215 – 245% and 450 – 740% for the 100 and 300 mg/day CNF doses, respectively. Assuming a fraction unbound in plasma of 0.01 (Devineni et al., 2013), the corresponding maximum unbound concentrations of CNF in plasma are 0.03 and 0.11 µM, respectively, both of which are lower than the range of $K_{i,u}$ values observed for CNF inhibition of UGT1A1 and UGT1A9. Although it is expected that the unbound concentration of the inhibitor in blood reflects the drug concentration in hepatocytes, we and others have observed previously that optimal prediction of DDI potential arising from inhibition of UGT and cytochrome P450 enzymes is obtained using total perpetrator drug concentration (Ito et al., 2004; Brown et al., 2005; Rowland et al., 2006; Raungrut et al., 2010). Thus, inhibition of UGT1A1 and UGT1A9 by CNF in vivo cannot be discounted. However, it is likely that the magnitude of the predicted increases in the AUC-ratios based on maximum plasma CNF concentrations may be over-estimated, especially since there appears to be no evidence for the development of jaundice

(arising from inhibition of UGT1A1-catalyzed bilirubin glucuronidation) in patients taking CNF.

The mean maximum plasma concentration of DPF (10 mg/day) at steady-state is reported as 169 µg/L (0.41 µM) and the unbound fraction in plasma as 0.09 (Kasichayanula et al., 2014; Plosker 2012), providing a maximum unbound concentration of 0.04 µM. Thus, both the maximum total and unbound DPF concentrations are low compared to the $K_{i,u}$ values for inhibition of UGT1A1 and UGT1A9. Interestingly, however, co-administration of the known UGT1A9 inhibitor mefenamic acid (Gaganis et al, 2007) increased the area under the plasma concentration – time curve of DPF in healthy subjects by 51% (Kasichayanula et al., 2013).

CNF has been reported not to alter the clearance of co-administered acetaminophen (Ivokana, Product Information, 2013), a drug cleared predominantly by UGT1A6 (with lesser contributions of UGT 1A1 and 1A9) (Miners et al., 2011). As discussed above, DPF is not predicted to inhibit UGT1A9, but a potential effect of CNF on UGT1A1 and UGT1A9-catalyzed drug glucuronidation cannot be discounted. Moreover, it is conceivable that CNF may inhibit renal UGT1A9 activity in vivo to a greater extent than predicted from the $[I]/K_{i,u}$ ratio. We have demonstrated that basolateral uptake of 4MU in the isolated rat perfused kidney is high, resulting in extensive renal 4MU glucuronidation (Wang et al., 2010). Thus, the intra-renal concentration of drugs such as CNF (and DPF) may be higher than in plasma, resulting in a larger than expected $[I]/K_{i,u}$ ratio. Importantly, UGT1A9 is the predominant UGT protein expressed in the kidney (Margaillan et al., 2015), consistent

DMD Fast Forward. Published on July 15, 2015 as DOI: 10.1124/dmd.115.065870
This article has not been copyedited and formatted. The final version may differ from this version.

with the observation that numerous UGT1A9 substrates are glucuronidated by this organ (in vitro and/or in vivo) (Knights and Miners, 2010). Indeed, available data suggests that renal glucuronidation contributes significantly to DPF metabolic clearance (Kasichayanula et al., 2012), and UGT1A9-catalyzed frusemide glucuronidation in the kidney appears to be the primary metabolic pathway of this drug in humans (Smith and Benet, 1983; Kerdpin et al., 2008).

Although it has been reported that UGT2B4 contributes to CNF glucurondation (see Introduction), CNF inhibition of this enzyme was negligible. Apart from UGT1A1 and UGT1A9, CNF inhibited UGT1A10 with similar potency to UGT1A9. Available evidence indicates that UGT1A10 is expressed exclusively in the gastrointestinal tract (Rowland et al., 2013). Since the focus of this study was to identify DDIs that would result in altered drug clearance, the inhibition of UGT1A10 was not characterized further.

In summary, CNF is a potent inhibitor of UGT1A1 and UGT1A9 in vitro, whereas DPF causes 'modest' inhibition of these enzymes. In vitro – in vivo extrapolation based on the $[I]/K_{i,u}$ ratios excludes DPF as a perpetrator of DDIs arising from inhibition of UGT enzymes, but inhibition of UGT1A1 and UGT1A9 by CNF in vivo cannot be discounted. Like CNF and DPF, other SGLT2 inhibitors in clinical development (or entering clinical practice) contain a glycoside moiety, which is presumably an important structural feature for CNF and DPF binding to UGT enzymes. Thus, the screening of SGLT2 inhibitors for effects on UGT enzymes is warranted in order to identify or exclude potential DDIs.

AUTHORSHIP CONTRIBUTIONS

Participated in research design: Pattanawongsa, Miners, Rowland

Conducted experiments: Pattanawongsa

Performed data analysis: Pattanawongsa, Miners, Chau

Wrote or contributed to the writing of the paper: Pattanawongsa, Miners

REFERENCES

American Diabetes Association (2012) Standards of medical care in diabetes – 2012. *Diabetes Care* **35**(supplement 1):S11-S63.

Australian Medicines Handbook (2014) Drugs for diabetes. Australian Medicines Handbook Pty Ltd, pp 408-422.

Boase S, Miners JO (2002) In vitro – in vivo correlations for drugs eliminated by glucuronidation: Investigations with the model substrate zidovudine. *Br J Clin Pharmacol* **54:**493-503.

Brown HS, Ito K, Galetin A, and Houston JB (2005) Prediction of in vivo drug-drug interactions from in vitro data: Impact of incorporating parallel metabolic pathways of drug elimination and inhibitor absorption rate constant. *Br J Clin Pharmacol* **60:**508-518.

Devineni D, Curtin CR, Polidori D, Gutierrez MJ, Murphy J, Rusch S, and Rothenberg PL (2013) Pharmacokinetics and pharmacodynamics of canagliflozin, a sodium-glucose co-transporter 2 inhibitor, in subjects with type 2 diabetes. *J Clin Pharmacol* **53:**601-610.

Gaganis P, Miners JO, and Knights KM (2007) Glucuronidation of fenemates: Kinetic studies using human kidney cortical microsomes and recombinant UDP-glucuronosyltransferase (UGT) 1A9 and 2B7. *Biochem Pharmacol* **73:**1683-1691.

Gill KL, Houston JB, and Galetin A (2012) Characterization of in vitro glucuronidation clearance of a range of drugs in human kidney microsomes: Comparison with liver and intestinal glucuronidation and impact of albumin. *Drug Metab Dispos* **40:**825-835.

International Diabetes Foundation (2014) IDF Diabetes Atlas. www.idf.org/diabetesatlas/update-2014.

Ito K, Iwatsubo T, Kanamitsu S, Ueda K, Suzuki H, and Sugiyama Y (1998) Prediction of pharmacokinetic alterations caused by drug-drug interactions: Metabolic interaction in the liver. *Pharmacol Ther* **50:**387-411.

Ito K, Brown HS, and Houston JB (2004) Database analyses for the prediction of in vivo drug-drug interactions from in vitro data. *Br J Clin Pharmacol* **57:**473-486.

Kasichayanula S, Liu X, Benito MP, Yao M, Pfister M, LaCreta F, Humphreys WG, and Boulton DW (2012) The influence of kidney function on dapagliflozin exposure, metabolism and pharmacodynamics in healthy subjects and in patients with type 2 diabetes mellitus. *Br J Clin Pharmacol* **76:**432-434.

Kasichayanula S, Liu X, Griffen SC, LaCreta F, and Boulton DW (2013) Effects of rifampin and memfenamic acid on the pharmacokinetics of dapagliflozin. *Diabetes Obes Metab* **15:**280-283.

Kasichayanula S, Liu X, LaCreta F, Griffen SC, and Boulton DW (2014) Clinical pharmacokinetics and pharmacodynamics of dapaliflozin, a selective inhibitor of sodium-glucose co-transporter type 2. *Clin Pharamcokinet* **53:**17-27.

Kerdpin O, Knights KM, Elliot DJ, and Miners JO (2008) In vitro characterization of human renal and hepatic frusemide glucuronidation and identification of the UDP-glucuronosyltransfearse enzymes involved in this pathway. *Biochem Pharmacol* **76:**249-257.

Kinne RKH and Castaneda F (2011) SGLT inhibitors as new therapeutic tools in the treatment of diabetes. In, Diabetes – Perspectives in Drug Therapy, *Handbook of Experimental Pharmacology* (ed Schwanstecher M) **203:**105-126.

Knights KM and Miners JO (2010) Renal UDP-glucuronosyltransferases and the glucuronidation of xenobiotics and endogenous compounds. *Drug Metab Rev* **42:**60-70.

Lewis BC, Mackenzie PI, Elliot DJ, Burchell B, Bhasker CR and Miners JO (2007) Amino terminal domains of human UDP-glucuronosyltransferases (UGT) 2B7 and 2B15 associated with substrate selectivity and autoactivation. *Biochem Pharmacol* **73:**1463-1473.

Mamidi RNVS, Cuyckens F, Chen J, Scheers E, Kalamaridis D, Lin R, Silva J, Sha S, Evans DC, Kelley MF, Devineni D, Johnson MD, and Lim HK (2014) Metabolism and excretion of canagliflozin in mice, rats, dogs and humans. *Drug Metab Dispos* **42:**903-916.

Manevski N, Moreolo PS, Yi-Kauhalouma, and Finel M (2011) Bovine serum albumin decreases K_m values of human UDP-glucuronosyltransferases 1A9 and 2B7 and increases V_{max} values of UGT1A9. *Drug Metab Dispos* **39:**2117-2129.

Margaillan G, Rouleau M, Fallon JK, Caron P, Villeneuve L, Turcotte V, Smith PC, Joy MS, and Gullemette C (2015) Quatitative profiling of human renal UGTs *and glucuronidation activity: A comparison of normal and tumoral kidney tissues. Drug Metab Dispos* **43:**611-615.

McLure JA, Miners JO, and Birkett DJ (2000) Nonspecific binding of drugs to human liver microsomes. *Br J Clin Pharmacol* **49:**453-461.

Miners JO, Mackenzie PI and Knights KM (2010a) The prediction of drug glucuronidation parameters in humans: UDP-glucuronosyltransferase enzyme selective substrate and inhibitor probes for reaction phenotyping and in vitro – in vivo extrapolation of drug clearance and drug-drug interaction potential. *Drug Metab Rev* **42:**189-201.

Miners JO, Polasek TM, Mackenzie PI and Knights KM (2010b) The in vitro characterization of inhibitory drug-drug interactions involving UDP-glucuronosyltransferase. In, Enzyme and Transporter based drug-drug interactions

(Eds Pang KS, Rodrigues AD and Peter R), Chapter 8, pp 217-236, Springer (New York).

Miners JO, Bowalgaha K, Elliot DJ, Baranczewski P, and Knights KM (2011) Characterization of niflumic acid as a selective inhibitor of human liver microsomal UDP-glucuronosyltransferase 1A9: Application to the reaction phenotyping of acetaminophen glucuronidation. *Drug Metab Dispos* **39:**644-652.

Obermeier M, Yao M, Khanna A, Koplowitz B, Zhu M, Li W, Komoroski B, Kasichayanula S, Discenza L, Washburn W, Meng W, Ellsworth BA, Whaley JM, and Humphreys WG (2010) In vitro characterization and pharmacokinetics of dapagliflozin (BMS-512148), a potent sodium-glucose cotransporter type II inhibitor, in animals and humans. *Drug Metab Dispos* **38:**405-414.

Plosker GL (2012) Dapagliflozin: A review of its use in type diabetes mellitus. *Drugs* **72:**2289-2312.

Raungrut P, Uchaipichat V, Elliot DJ, Janchawee B, Somogyi AA and Miners JO (2010) In vitro – in vivo extrapolation predicts drug-drug interactions arising from inhibition of codeine glucuronidation by dextropropoxyphene, fluconazole, ketoconazole and methadone in humans. *J Pharmacol Exp Ther* **334:**609-618.

Rowland A, Elliot DJ, Williams JA, Mackenzie PI, Dickinson RG, and Miners JO (2006) In vitro characterization of lamotrigine N2-glucuronidation and the lamotrigine – valproic acid interaction. *Drug Metab Dispos* **34:**1304-1311.

Rowland A, Gaganis P, Elliot DJ, Mackenzie PI, Knights KM, and Miners JO (2007) Binding of inhibitory fatty acids is responsible for the enhancement of UDP glucuronosyltransferase 2B7 activity by albumin: Implications for in vitro-in vivo extrapolation. *J Pharmacol Exp Ther* **321:**137–147.

Rowland A, Knights KM, Mackenzie PI and Miners JO (2008) "Albumin effect" and drug glucuronidation : Bovine serium albumin and fatty acid-free human serum albumin enhance the glucuronidation of UDP-glucurososyltransferase (UGT) 1A9 but not UGT1A1 and UGT1A6 activities. *Drug Metab Disp* **36:**1056-1062.

Rowland A, Miners JO, and Mackenzie PI (2013) The UDP-glucuronosyltransferases: Their role in drug metabolism and detoxification. *Int J Biochem Cell Biol* **45:**1121-1132.

Scheen AJ (2014) Evaluating SGLT2 inhibitors for type 2 diabetes: Pharmacokinetic and toxicological considerations. *Expert Opin Drug Metab Toxicol* **10:**647-663.

Smith DE and Benet LZ (1983) Biotransformation of furosemide in kidney transplant patients. *Eur J Clin Pharmacol* **24:**787-790.

Stenlof K, Cefalu WT, Kim, K-A, Alba M, Usikin K, Tong C, Canovatchel W, and Meininger G (2013) Efficacy and safety of canagliflozin monotherapy in subjects with type 2 diabetes mellitus inadequately controlled with diet and exercise. *Diabetes, Obesity and Metabolism* **15:**372-382.

Uchaipichat V, Mackenzie PI, Guo X-H, Gardner-Stephen D, Galetin A, Houston JB and Miners JO (2004) Human UDP-glucuronosyltransferases: Isoform selectivity and kinetics of 4-methylumbelliferone and 1-naphthol glucuronidation, effects of organic solvents, and inhibition by diclofenac and probenecid. *Drug Metab Disp* **32:**413-23.

Uchaipichat V, Mackenzie PI, Elliot DJ and Miners JO (2006a) Selectivity of substrate (trifluopeazine) and inhibitor (amitriptyline, androsterone, canrenoic acid, hecogenin, phenylbutazone, quinidine, quinine, and sulfinpyrazone) probes for human UDP-glucuronosyltransferases. *Drug Metab Disp* **34:**449-456.

Uchaipichat V, Winner LK, Mackenzie PI, Elliot DJ, Williams JA and Miners JO (2006b) Quantitative prediction of in vivo inhibitory interactions involving glucuronidated drugs from in vitro data: The effect of fluconazole on zidovudine glucuronidation. *Br J Clin Pharmacol* **61:**427-439.

Udomuksorn W, Elliot DJ, Lewis BC, Mackenzie PI, Yoovathaworn K and Miners JO (2007) Influence of mutations associated with Gilbert and Crigler-Najjar type II syndromes on glucuronidation kinetics of bilirubin and other UDP-glucuronosyltransferases 1A substrates. *Pharmacogenet Genomics* **17:**1017-1029.

Vasilakou D, Karagiannis T, Athanasiadou M, Liakos A, Bekiari E, Sarigianni M, Matthews DR, and Tsapas (2013) Sodium-glucose cotransporter 2 inhibitors for type 2 diabetes: A systematic review and meta-analysis. *Ann Intern Med* **159:**262-274.

Walsky RL, Bauman JN, Bourcire K, Giddens G, Lapham K, Negahban A, Ryder TF, Obach RS, Hyland R, and Goosen TC (2012) Optimized assays for human UDP-glucuronosyltransferase (UGT) activities: Altered alamethicin concentration and utility to screen for UGT inhibitors. *Drug Metab Dispos* **40:**1051-1065.

FOOTNOTE

AP is funded by a post-graduate research scholarship from Flinders University.

DMD Fast Forward. Published on July 15, 2015 as DOI: 10.1124/dmd.115.065870
This article has not been copyedited and formatted. The final version may differ from this version.

FIGURE LEGENDS

Figure 1. Structures of canagliflozin and dapagliflozin. Arrows show sites of glucuronidation.

Figure 2. Inhibition of recombinant human UGT enzymes by canagliflozin and dapagliflozin. Bars represent the mean of duplicate estimates (< 5% variance).

Figure 3. Dixon plots for canagliflozin inhibition of the enzyme/substrate pairs: (A) UGT1A1/β-EST; (B) HLM/β-EST; (C) UGT1A9+BSA/4MU; (D) UGT1A9+BSA/PRO; (E) HLM+BSA/PRO. Concentrations of canagliflozin and substrates are corrected for binding to the respective enzyme sources and BSA (0.5 % w/v). Points are experimentally derived values (mean of duplicate estimates; < 5% variance), while lines are from fitting with equations 1 (UGT1A9) or 4 (UGT1A1).

Figure 4. Dixon plots for dapagliflozin inhibition of the enzyme/substrate pairs: (A) UGT1A1/β-EST; (B) HLM/β-EST; (C) UGT1A9+BSA/4MU; (D) UGT1A9+BSA/PRO; (E) HLM+BSA/PRO. Concentrations of dapagliflozin and substrates are corrected for binding to the respective enzyme sources and BSA (1 % w/v). Points are experimentally derived values (mean of duplicate estimates; < 5% variance), while lines are from fitting with equations 1 (UGT1A9) or 4 (UGT1A1).

DMD Fast Forward. Published on July 15, 2015 as DOI: 10.1124/dmd.115.065870
This article has not been copyedited and formatted. The final version may differ from this version.

Table 1. Derived $K_{i,u}$ values for canagliflozin and dapaliflozin inhibition of recombinant and human liver microsomal UGT1A1 and UGT1A9.

Enzyme source / substrate	$K_{i,u}$ (μM)[a]	
	CNF	DPF
UGT1A1 / β-estradiol	7.2 ± 1.4	81 ± 1.4
HLM / β-estradiol	9.1 ± 0.2	81 ± 3.8
UGT1A9 / 4-MU	1.4 ± 0.1	11 ± 0.5
UGT1A9 / propofol	2.9 ± 0.1	12 ± 0.6
HLM / propofol	3.0 ± 0.1	15 ± 0.6

[a] ± standard error of parameter fit

DMD Fast Forward. Published on July 15, 2015 as DOI: 10.1124/dmd.115.065870

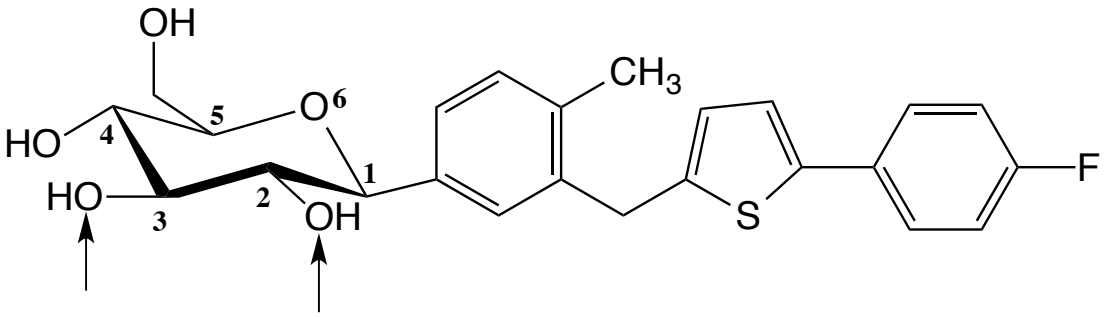

Canagliflozin

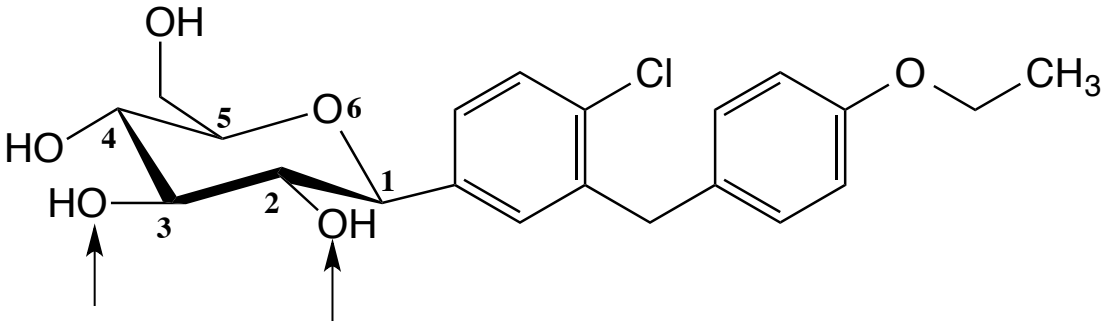

Dapagliflozin

Figure 1

Figure 2

DMD Fast Forward. Published on July 15, 2015 as DOI: 10.1124/dmd.115.065870
This article has not been copyedited and formatted. The final version may differ from this version.

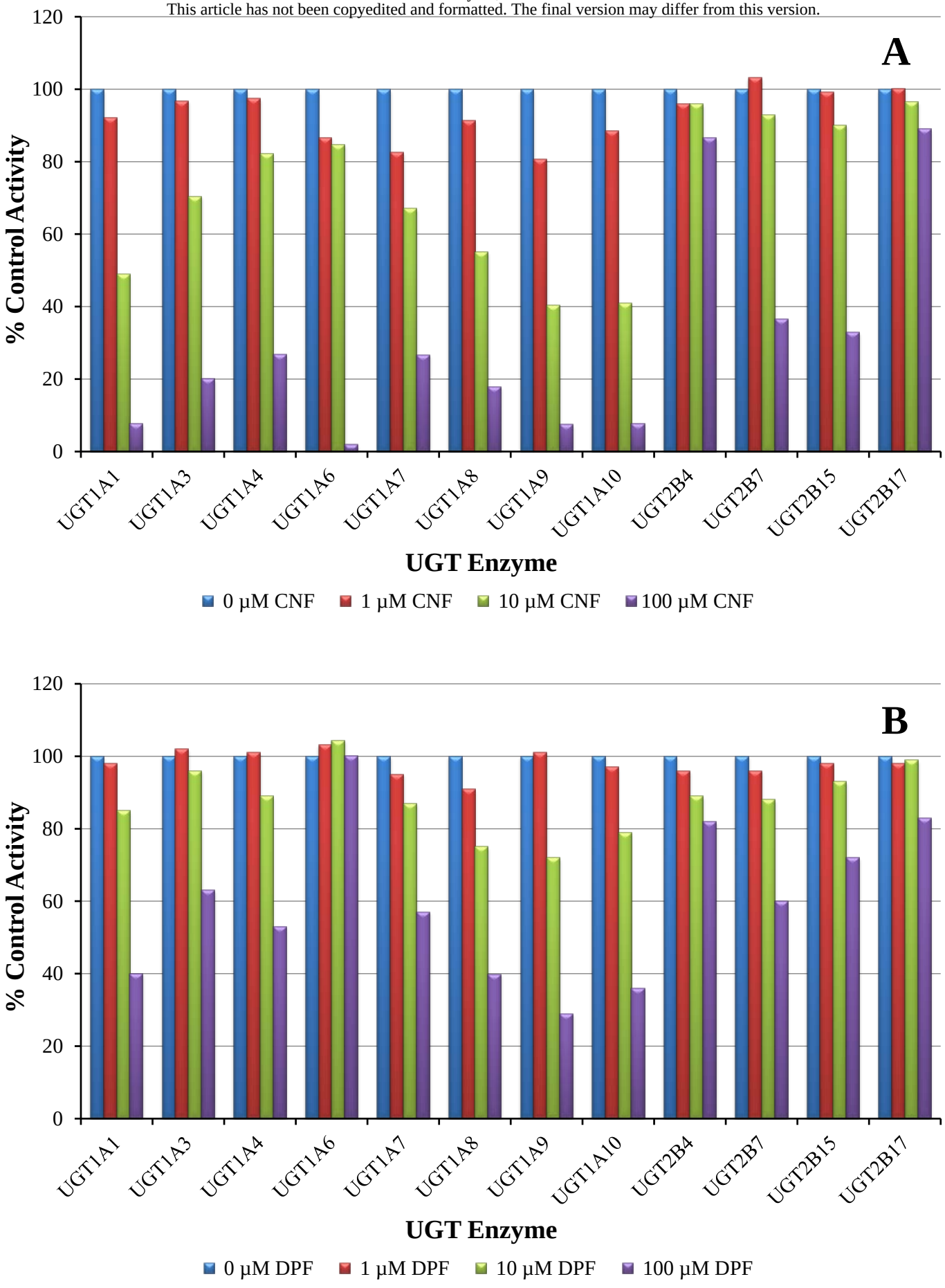

DMD Fast Forward. Published on July 15, 2015 as DOI: 10.1124/dmd.115.065870
This article has not been copyedited and formatted. The final version may differ from this version.

Figure 3

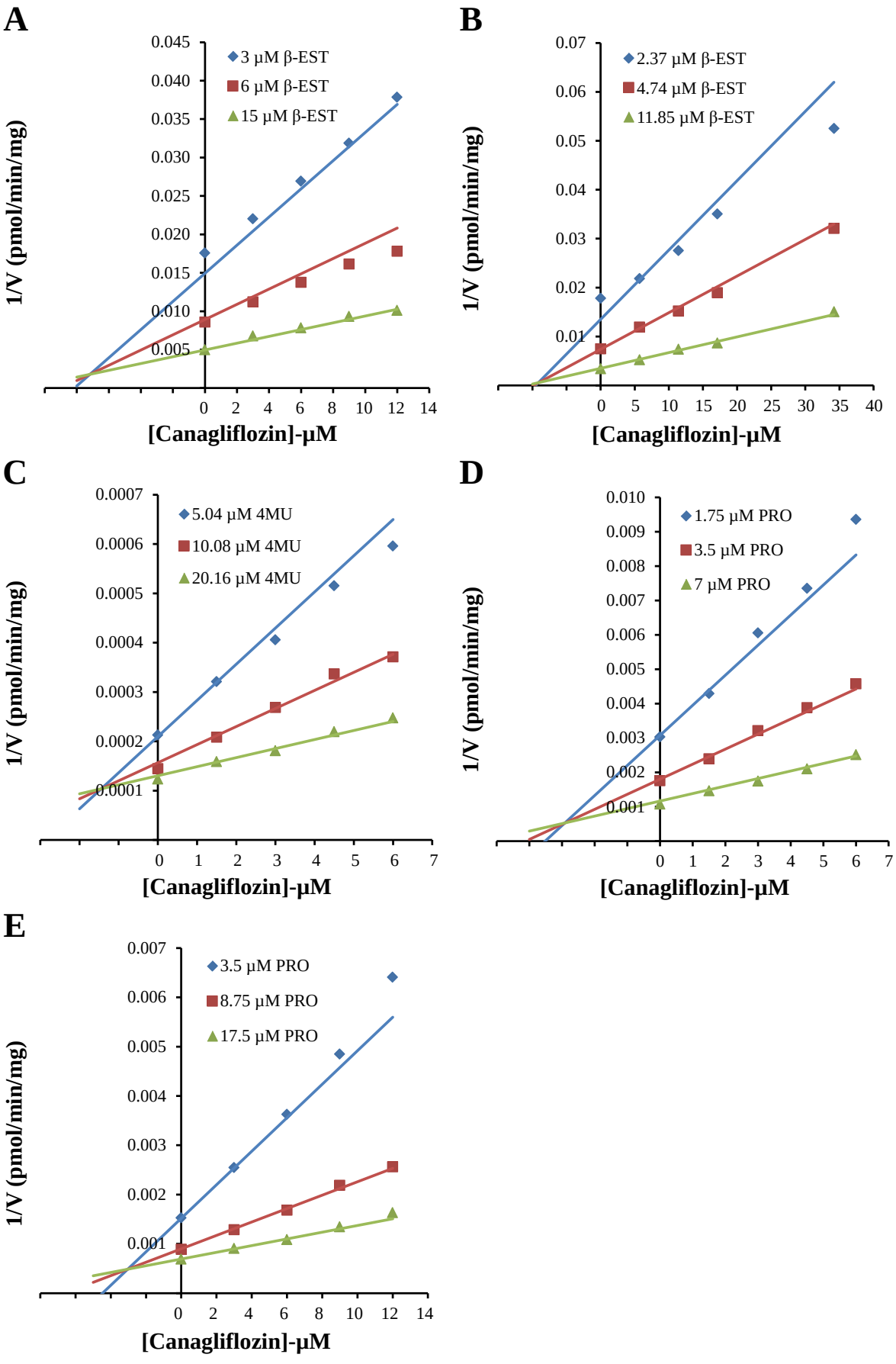

DMD Fast Forward. Published on July 15, 2015 as DOI: 10.1124/dmd.115.065870
This article has not been copyedited and formatted. The final version may differ from this version.

Figure 4

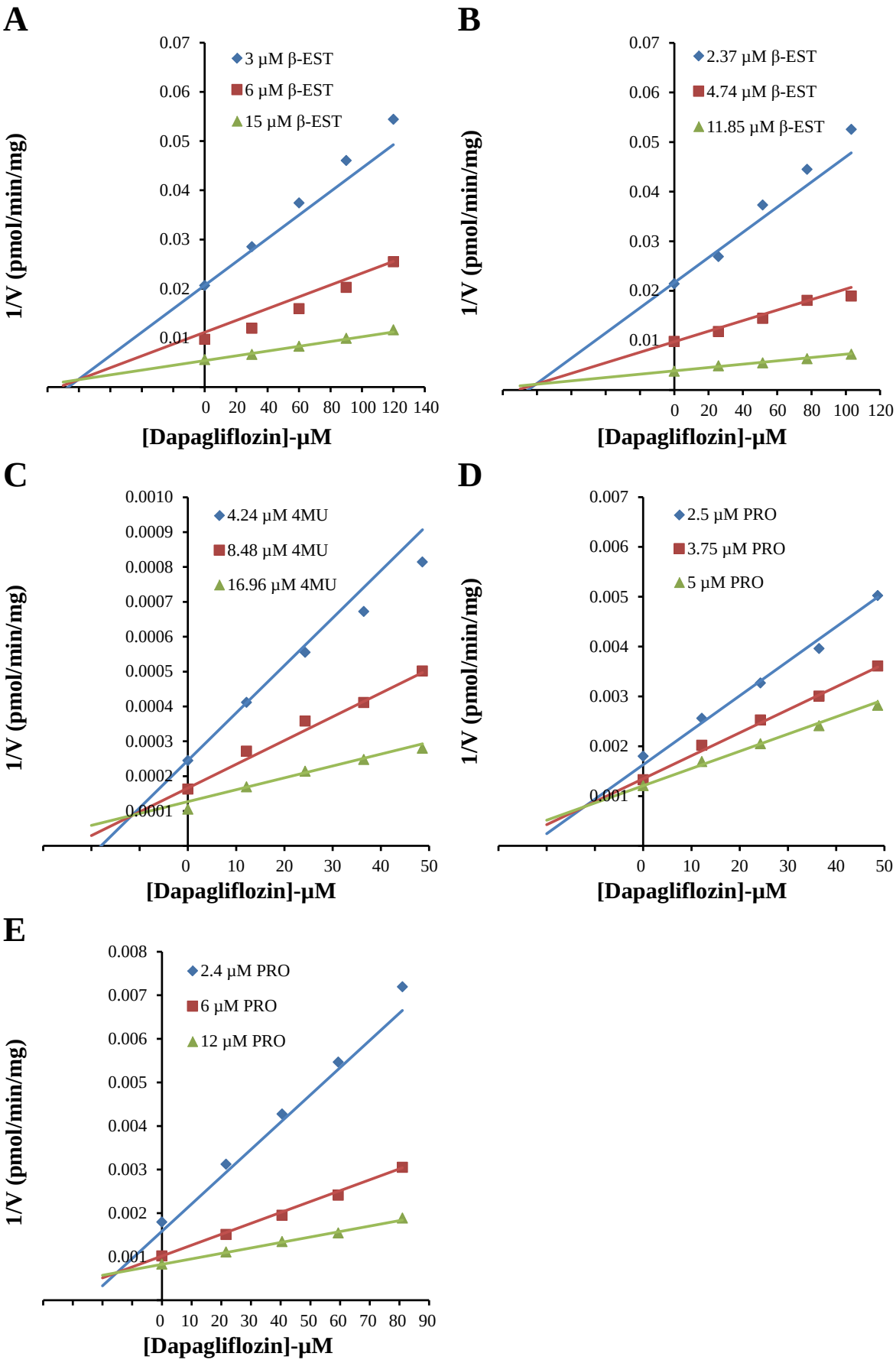

Supplemental Tables 1 to 6. Attarat Pattanawongsa, Nuy Chau, Andrew Rowland and John O. Miners. The inhibition of human UDP-glucuronosyltransferase (UGT) enzymes by canagliflozin and dapagliflozin: Implications for drug-drug interactions. Drug Metabolism and Disposition.

Supplemental Table 1. Binding of dapagliflozin to protein sources (HEK cell lysate and HLM) in the absence and presence of BSA (1% w/v). Binding is expressed as the fraction unbound in the incubation medium (fu_{inc}).

Concentration (μM)	Protein source	fu_{inc}
10, 50, 100, 200	HEK (0.25 mg/ml)	0.94 ± 0.02
10, 50, 100, 200, 500, 1000	HLM (0.25 mg/ml)	0.86 ± 0.03
10, 50, 100, 200	HEK (0.025 mg/ml) + 1%BSA	0.27 ± 0.03
10, 50, 100, 200	HEK (0.25 mg/ml) + 1%BSA	0.30 ± 0.01
10, 50, 100, 200, 500, 1000	HLM (0.5 mg/ml) + 1%BSA	0.29 ± 0.02
10 and 200 (50 μM 4MU added)	HEK (0.025 mg/ml) + 1%BSA	0.29 ± 0.03
10 and 200 (20 μM β-EST added)	HLM (0.25 mg/ml)	0.85 ± 0.01
10 and 200 μM (50 μM PRO added)	HEK (0.25 mg/ml) + 1%BSA	0.29 ± 0.02
10 and 400 μM (50 μM PRO added)	HLM (0.5 mg/ml) + 1%BSA	0.30 ± 0.04

Supplemental Table 2. Binding of canagliflozin to protein sources (HEK cell lysate and HLM) in the absence and presence of BSA (0.5% w/v). Binding is expressed as the fraction unbound in the incubation medium (fu_{inc}).

Concentration (μM)	Protein source	fu_{inc}
2.5, 10, 25, 50, 100	HEK (0.25 mg/ml)	0.96 ± 0.09
2.5, 10, 50, 100, 200	HLM (0.25 mg/ml)	0.38 ± 0.02
2.5, 10, 25, 50, 100	HEK (0.025 mg/ml) + 0.5%BSA	0.10 ± 0.01
2.5, 10, 25, 50, 100	HEK (0.25 mg/ml) + 0.5%BSA	0.10 ± 0.01
2.5, 10, 25, 50, 100, 200	HLM (0.5 mg/ml) + 0.5%BSA	0.08 ± 0.01
10 and 100 μM (50 μM 4MU added)	HEK (0.025 mg/ml) + 0.5%BSA	0.09 ± 0.00
10 and 100 μM (20 μM β-EST added)	HLM (0.25 mg/ml)	0.40 ± 0.03
10 and 100 μM (10 μM PRO added)	HEK (0.25 mg/ml) + 0.5%BSA	0.12 ± 0.01
10 and 100 μM (50 μM PRO added)	HLM (0.5 mg/ml) + 0.5%BSA	0.08 ± 0.02

Supplemental Table 3. Binding of 4-methylumbelliferone to HEK cell lysate in the presence of BSA (0.5 and 1% w/v). Binding is expressed as the fraction unbound in the incubation medium (fu_{inc}).

Concentration (μM)	Protein source	fu_{inc}
5, 10, 20, 50	HEK (0.025 mg/ml) + 0.5%BSA	0.66 ± 0.01
5, 10, 20, 50	HEK (0.025 mg/ml) + 1%BSA	0.52 ± 0.01
5 and 50 (200 μM DPF added)	HEK (0.025 mg/ml) + 1%BSA	0.53 ± 0.02
5 and 50 (100 μM CNF added)	HEK (0.025 mg/ml) + 0.5%BSA	0.68 ± 0.02

Supplemental Table 4. Binding of propofol to protein sources (HEK cell lysate and HLM) in the presence of BSA (0.5 and 1% w/v). Binding is expressed as the fraction unbound in the incubation medium (fu_{inc}).

Concentration (μM)	Protein source	fu_{inc}
2, 4, 8, 10	HEK (0.25 mg/ml)+0.5%BSA	0.34 ± 0.03
10, 50, 100, 200	HEK (0.25 mg/ml)+1%BSA	0.24 ± 0.02
5, 10, 50, 100	HLM (0.5 mg/ml)+0.5%BSA	0.32 ± 0.05
5, 10, 50, 100	HLM (0.5 mg/ml)+1%BSA	0.21 ± 0.02
2 and 10 (100 μM CNF added)	HEK (0.25 mg/ml)+0.5%BSA	0.36 ± 0.01
5 and 50 (200 μM CNF added)	HLM (0.5 mg/ml)+0.5%BSA	0.34 ± 0.01
5 and 50 (200 μM DPF added)	HEK (0.25 mg/ml)+1%BSA	0.25 ± 0.03
5 and 50 (400 μM DPF added)	HLM (0.5 mg/ml)+1%BSA	0.23±0.03

Supplemental Table 5. Binding of β-estradiol to HEK cell lysate and HLM. Binding is expressed as the fraction unbound in the incubation medium (fu_{inc}).

Concentration (μM)	Protein source	fu_{inc}
2, 5, 10, 20	HEK (0.25 mg/ml)	1.01 ± 0.07
2, 5, 10, 20	HLM (0.25 mg/ml)	0.79 ± 0.05
2 and 20 (200 μM DPF added)	HLM (0.25 mg/ml)	0.82 ± 0.03
2 and 20 (100 μM CNF added)	HLM (0.25 mg/ml)	0.80 ± 0.03

Supplemental Table 6. HPLC conditions for the quantification of canagliflozin, dapagliflozin, β-estradiol, 4-methylumbelliferone and propofol in dialysates from equilibrium dialysis experiments.

Drug	Mobile phase composition	Gradient elution time (min)	Detector wavelength (nm)	Retention time (min)
Isocratic elution				
Dapagliflozin	65%A : 35%D	-	236	3.2
Canagliflozin	60%A : 40%D	-	291	3.9
4-Methylumbelliferone	80%B : 20%D	-	316	2.7
Propofol	30%C : 70%D	-	214	2.3
β-Estradiol	60%B : 40%D	-	220	2.9
Gradient elution				
4-Methylumbelliferone (in the presence of canagliflozin)	80%B : 20%D 20%B : 80%D 20%B : 80%D 80%B : 20%D	0 1.5 3.5 4	316	2.7 (4-MU) 4.8 (CNF)
Canagliflozin (in the presence of β-estradiol)	70%A : 30%D 50%A : 50%D 50%A : 50%D 70%A : 30%D	0 5 5.5 6.5	291	5.9 (CNF) 5.4 (β-EST)
β-Estradiol (in the presence of canagliflozin)	80%B : 20%D 60%B : 40%D 60%B : 40%D 80%B : 20%D	0 7 7.5 8.5	220	7.9 (β-EST) 8.9 (CNF)

Column: Nova-Pak® Waters, C18, 3.9 x 150 mm, 4 µm particle size.

Mobile phase composition:

A: 5% acetonitrile in water.

B: 10 mM triethylamine (adjusted to pH 2.5 with 12 M perchloric acid) containing 10% acetonitrile.

C: 5 mM ammonium acetate (adjusted to pH 4.6 with glacial acetic acid) containing 5% acetonitrile.

D: acetronitrile.